

**Supplementary Information: Photonic Architectures for
Equilibrium High-Temperature Bose-Einstein Condensation in
Dichalcogenide Monolayers**

Jian-Hua Jiang^{1,*} and Sajeew John¹

*¹Department of Physics, University of Toronto,
Toronto, Ontario, M5S 1A7 Canada*

* jianhua.jiang.phys@gmail.com

GUIDED 2D PHOTONIC BAND EDGE

In the woodpile PC cavity the lowest 2D photonic band has two dispersion minima: the X point $\vec{Q}^{(X)} = (\frac{\pi}{a}, 0, 0)$ and the Y point $\vec{Q}^{(Y)} = (0, \frac{\pi}{a}, 0)$. The dispersion has a C_{4v} symmetry, inherited from the D_{2d} symmetry of the woodpile PC cavity. We consider the situation when the 2D photonic band edge is close to the exciton emission energy (i.e., $a = 380$ nm) where the dispersion of the 2D photonic band near the minima $\nu = X, Y$ is $\hbar\omega_{\vec{q}} = \hbar\omega_0 + \frac{\hbar^2(q_x - Q_x^{(\nu)})^2}{2m_x^{(\nu)}} + \frac{\hbar^2(q_y - Q_y^{(\nu)})^2}{2m_y^{(\nu)}}$. Here, $m_x^{(X)} = m_y^{(Y)} \simeq 2.4 \times 10^{-5}m_0$ and $m_x^{(Y)} = m_y^{(X)} \simeq 7.2 \times 10^{-5}m_0$ where m_0 is the bare electron mass in vacuum. In SP PC cavity the dispersion of the lowest 2D photonic band has the C_{2v} symmetry. There is only one dispersion minimum at the Y point where the effective mass is also anisotropic with $m_x = 5.7 \times 10^{-5}m_0$ and $m_y = 2.1 \times 10^{-5}m_0$ for $a = 370$ nm. The effective mass of photon in the FP cavity is $0.68 \times 10^{-5}m_0$ at exciton-photon resonance.

ELECTRONIC BAND STRUCTURE OF MOSE₂

Schematic of electronic band structure of MoSe₂ monolayer is shown in Fig. 3a in the main text. Band extrema are located at the $\mathbf{K} = (\frac{4\pi}{3a_s}, 0)$ (a_s is the honeycomb lattice constant of MoSe₂) and $-\mathbf{K}$ points[1]. Very large splitting occurs between spin-up and -down states of 180 meV[2] in the valence band due to spin-orbit interaction. Denoting the z -components of total, orbital and spin angular momenta as J_z , L_z and S_z , the valence band maximum at the \mathbf{K} valley gives spin-up $J_z = \frac{3}{2}\hbar$ holes (absence of an electron with $L_z = -\hbar$ and $S_z = -\frac{1}{2}\hbar$ in the valence band). Its time-reversal partner $-\mathbf{K}$ valley gives spin-down $J_z = -\frac{3}{2}\hbar$ holes. This special electronic band structure leads to optical selection rules for the lowest excitonic states (see Fig. 3a in the main text): the σ_+ photon excites only spin-up $J_z = \frac{3}{2}\hbar$ hole and spin-down $(J_z, L_z, S_z) = (-\frac{1}{2}\hbar, 0, -\frac{1}{2}\hbar)$ electron in the \mathbf{K} valley, while σ_- photon excites only spin-down $J_z = -\frac{3}{2}\hbar$ hole and spin-up $(J_z, L_z, S_z) = (\frac{1}{2}\hbar, 0, \frac{1}{2}\hbar)$ electron in the $-\mathbf{K}$ valley[1].

ESTIMATION OF THE EXCITON-PHOTON COUPLING IN MOSE₂

From Ref. [3] the imaginary part of the optical susceptibility at the energy of the 1s-exciton state $E_{X0} = \hbar\omega_{X0}$ is given by

$$\text{Im}[\chi(\omega_{X0})] = \frac{2d_{cv}^2|\phi(0)|^2}{L_c\hbar\delta}, \quad (1)$$

where L_c is the quantum well width and $\hbar\delta$ is the homogeneous broadening of the 1s-exciton state. From measurements of $\text{Im}[\chi(\omega_{X0})]$ we deduce $d_{cv}|\phi(0)|$.

The absorptance for an isolated two-dimensional system with thickness L_c is

$$\alpha = \frac{\omega L_c \text{Im}[\chi(\omega)]}{n\varepsilon_0 c}, \quad (2)$$

where ω and c are the frequency and speed of light, respectively, and n is the refractive index. From Ref. [4] the in-plane dielectric constant is 4.7 for a monolayer MoSe₂. Accordingly, we choose the refractive index $n \simeq 2.2$.

For MoSe₂ the absorptance $\alpha \simeq 6\%$ [5]. It follows from Eqs. (1) and (2) that

$$d_{cv}|\phi(0)| = \sqrt{\frac{0.06n\varepsilon_0\hbar\delta}{2\omega_{X0}}}. \quad (3)$$

From Ref. [5] the homogeneous broadening at room-temperature is about 50 meV. Therefore, $d_{cv}|\phi(0)| \simeq 2.4 \times 10^{-20}$ C which is 2.4 times as large as that of excitons GaAs quantum-wells of width 3 nm ($\simeq 1.0 \times 10^{-20}$ C). Using $|\phi(0)| = \sqrt{2/(\pi a_B^2)}$ for the 2D exciton and the Bohr radius $a_B = 1.2$ nm[5], we estimate $d_{cv} = 3.6 \times 10^{-29}$ Cm. This is also comparable with[1] $d_{cv} = \sqrt{2}a_s t e / E_g = 3.4 \times 10^{-29}$ Cm where $a_s = 3.313$ Å[1] is the honeycomb lattice constant of MoSe₂, $t = 0.94$ eV[1] is the effective electron hopping parameter, $e = 1.602 \times 10^{-19}$ C is the electronic charge and $E_g = 2.1$ eV[5] is the electronic band gap of MoSe₂.

ULTRA-SHORT POLARITON RADIATIVE LIFETIME IN FABRY-PÉROT MICROCAVITIES

1D periodic microstructures can provide strong coupling to a single high-quality factor optical mode. However the concomitant strong coupling to degenerate leaky modes severely reduces the polariton radiative lifetime. Here, we simulate polariton radiative decay from a finite-size polariton condensate using an extended dipole at the center of a FP cavity by

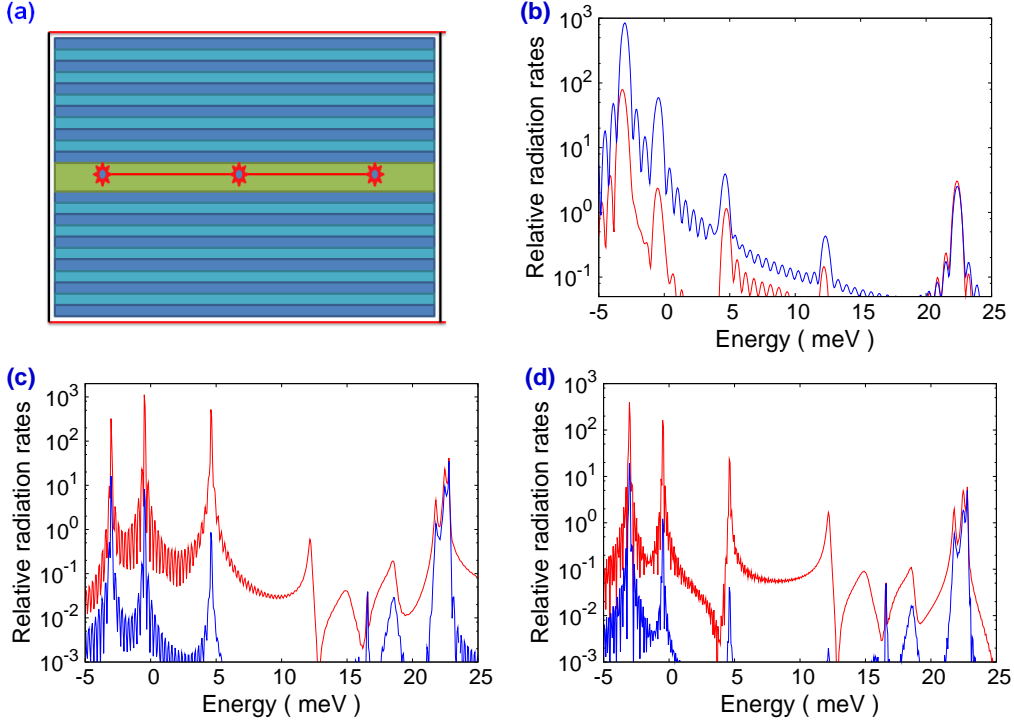


FIG. 1. Supplementary Figure S1. (a) Structure for 2D FDTD calculation of radiation rate in FP cavities. An extended dipole line source with length smaller than the width of the FP cavity is placed in the center (denoted by the line connecting the three star symbols). A Gaussian pulse excites dipole oscillations perpendicular to the paper plane causing outward radiation. The radiation flux is collected at the boundaries surrounding the cavity [denoted by the two red lines (top and bottom) and black lines (left and right)]. The radiation flux is calculated for the FP cavity as well as in the absence of the Bragg mirrors. The ratio of the former over the latter is plotted in (b)-(d). This ratio is resolved into escape through the top and bottom of the cavity (blue curves) and escape through the side directions (red curves). In the simulation, the width of the cavity is 14λ , while the length of the dipole is 12λ or 4λ . The structure is surrounded by an air region of thickness λ followed by perfectly matching layers of thickness 4λ . $\lambda = 0.8 \mu\text{m}$ is the length unit and hc/λ is equal to exciton emission energy $E_{X0} = 1.55 \text{ eV}$. (b)-(d): Dipole radiation rate in FP cavities relative to that in vacuum (red curves) as a function of the detuning of the dipole (exciton) energy from the Fabry-Pérot cavity mode energy. (b) FP cavity with 8 pairs of $\lambda/4$ SiO_2 and TiO_2 layers in the distributed Bragg mirrors above and below the $\lambda/2$ slab. (c) and (d) FP cavities with 15 pairs of $\lambda/4$ layers above and below the slab for different dipole sizes. Simulation is done via 2D FDTD with horizontal dipoles of lengths: (b) and (d) $9.6 \mu\text{m}$, (c) $3.2 \mu\text{m}$.

finite-difference-time-domain (FDTD). Different dipole sizes are used to represent small and large polariton BEC trap sizes. The radiative decay rate in the FP cavity is compared with that of the same dipole in vacuum (i.e., without the cavity). Experiments[6] suggest that the latter is about $1/(130 \text{ ps})$ in a MoSe_2 monolayer at room temperature. 2D FDTD simulations are used to provide a semi-quantitative prognosticator of a realistic 3D structure (see Fig. 1). The radiative decay rate (relative to that in vacuum) for SiO_2 - TiO_2 FP cavities with different dipole sizes and numbers of $\lambda/4$ layers are plotted as a function of the detuning of the dipole (exciton) energy from the Fabry-Pérot cavity energy in Fig. 1. The radiative decay is greatly enhanced at some energies while suppressed at other energies all within the exciton homogeneous line-width. The former are the hot-spots for exciton radiative decay leading to very short ($\lesssim 1 \text{ ps}$) polariton lifetime. In Fig. 1 the zero of energy $hc/\lambda = E_{X0} = 1.55 \text{ eV}$ and all energy scales in the figures are within the 1D photonic stop-gap at normal incidence.

For FP cavities with 8 pairs of $\lambda/4$ SiO_2 and TiO_2 layers (as in Fig. 1a) the cavity mode has a quality factor of 1.2×10^4 , implying a cavity photon lifetime of 11 ps. However, excitons can decay radiatively into a broad range of very low quality leaky modes. This radiative decay is most rapid into leaky modes with energy lower than the cavity mode. The 10^3 enhancement of radiation rate leads to sub-picosecond polariton lifetime. With 15 pairs of $\lambda/4$ layers the FP cavity mode has a quality factor as high as 1.8×10^6 implying a cavity photon lifetime of 1500 ps. As before, excitons can radiate through leaky modes (Figs. 1b and 1c) emerging from the sides of the FP. Radiation through leaky modes becomes weaker for the larger dipole size of 12λ than for the smaller dipole size of 4λ . Nevertheless, radiation lifetimes at the hot-spots are on the order of 1 ps. In the limit of an infinitely extended dipole contained in an FP cavity of infinite lateral extent, momentum conservation requires that all radiation is emitted into the cavity mode. However, in this case, BEC is excluded by the Mermin-Wagner theorem[8].

Dielectric disorder in realistic SiO_2 - TiO_2 FP's reduces the polariton lifetime even below our calculated time scales[9]. Moreover, at room temperature, excitons with energies away from strongly-coupled leaky modes but within the homogeneous linewidth (50 meV[5]) and phonon energy (43 meV[10]) can be scattered efficiently (within $\lesssim 1 \text{ ps}$) by phonons[11] to the leaky modes and then radiate rapidly. These effects reduce polariton lifetime to $\lesssim 1 \text{ ps}$ even for FP cavities with 15 pairs of $\lambda/4$ layers and cavity quality factor of 1.8×10^6 . The sub-picosecond lifetime of polaritons is still on the same order of magnitude

with the phonon scattering time (about 0.1 ps) in MoSe₂ at room temperature[11]. In contrast, in a 3D PBG microcavity architecture with a microcavity embedded in a 3D PBG material[12, 13], all leaky modes can be eliminated leading to very long polariton lifetime, limited only by exciton nonradiative decay. These nonradiative decay channels include Auger recombination arising from exciton-exciton collision and Shockley-Read-Hall recombination arising from electronic defects in the active semiconductor monolayers. Auger recombination is usually very inefficient in moderate to large band gap semiconductors such as MoSe₂ for the moderate exciton densities we consider (volume density less than 10¹⁸ cm⁻³)[7, 14]. Recently high (electronic) quality, large area MoSe₂ monolayers were successfully prepared by various methods[15–17], exploiting the significant mechanical, chemical and thermal stability of MoSe₂ monolayers[15]. In our architecture, the MoSe₂ monolayers are encapsulated by TiO₂ layers above and below, protecting them from defects introduced by wafer-fusion of the central slab to the photonic crystal. In well-fabricated samples, the polariton lifetime in our 3D PBG microcavities can be much longer than 130 ps, while efficient phonon scattering facilitates equilibration of the polariton gas in $\lesssim 1$ ps[11].

EFFECT OF EXCITON INHOMOGENEOUS AND HOMOGENEOUS BROADENING

As a result of polariton motional narrowing, inhomogeneous broadening within a given monolayer has only a minor effect on BEC[18–20]. Inhomogeneous broadening between different monolayers is modeled by a Gaussian random shift of the exciton emission energy in each monolayer, $E_{X0} \rightarrow E_{X0} + \delta E_l$, $l = 1, 2, 3$. The root mean square deviation of the vacuum Rabi splitting and the polariton dispersion depth V_{lp} , calculated as a function of exciton inhomogeneous broadening δE_{X0} , are shown in Fig. 2. The results for the three types of cavity are almost the same. The fluctuation of the vacuum Rabi splitting is considerably smaller than the exciton inhomogeneous broadening due to averaging among different monolayers[14], whereas the fluctuation of the dispersion depth V_{pl} is comparable to δE_{X0} . Nevertheless, for inhomogeneous broadening less than 10 meV, the dispersion depth remains larger than 48 meV enabling BEC up to 500 K (370 K) for the SP (woodpile) PC cavity.

Exciton homogeneous broadening is considerable in MoSe₂ at room temperature due to phonon scattering[11]. Optical measurements reveal a broadening of 50 meV in Ref. [5].

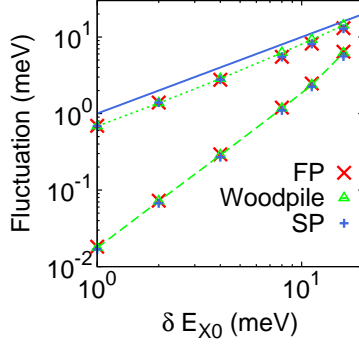


FIG. 2. Supplementary Figure S2. Root mean square deviation of the vacuum Rabi splitting (points linked by dotted curve) and the dispersion depth of polariton V_{lp} (points linked by dashed curve) as functions of the root mean square deviation of the exciton emission energy δE_{X0} when the detuning is $\Delta = 0$. The solid reference line denotes fluctuation equal to the exciton inhomogeneous broadening δE_{X0} .

Picosecond phonon scattering[11] facilitates thermal equilibration of polaritons within several picoseconds. Homogeneous broadening slightly degrades the vacuum Rabi splitting and the polariton dispersion depth. If the homogeneous broadening is described by a imaginary part of exciton energy, $i\Gamma$, the vacuum Rabi splitting is reduced from $2\hbar\Omega = 80$ meV to $2\sqrt{\hbar^2\Omega^2 - \Gamma^2/4} = 62$ meV at zero detuning for $\Gamma = 50$ meV. For a detuning of $\Delta = 40$ meV, exciton homogeneous broadening of $\Gamma = 50$ meV reduces the lower-polariton dispersion depth V_{lp} by 5.5 meV. The highest transition temperature is then reduced from 590 K to 560 K. If an inhomogeneous broadening of 30 meV is taken into account as well, the transition temperature will be reduced to 430 K which is still above room-temperature. This suggests that polaritons in woodpile and SP PC microcavities are robust against electronic and photonic disorder and exciton homogeneous broadening, enabling above room-temperature polariton BEC in realistic systems.

-
- [1] Xiao D., Liu, G.-B., Feng, W., Xu, X. & Yao, W. Coupled spin and valley physics in monolayers of MoS₂ and other group-VI dichalcogenides. *Phys. Rev. Lett.* **108**, 196802 (2012).
 - [2] Ross, J. S. *et al.* Electrical control of neutral and charged excitons in a monolayer semiconductor. *Nat. Commun.* **4**, 1474 (2013).

- [3] Haug, H. & Koch, S. W. *Quantum theory of the optical and electronic properties of semiconductors*, Chap. 10, (World Scientific, 2009).
- [4] Ramasubramaniam, A. Large excitonic effects in monolayers of molybdenum and tungsten dichalcogenides. *Phys. Rev. B* **86**, 115409 (2012).
- [5] Ugeda, M. M. *et al.* Observation of giant bandgap renormalization and excitonic effects in a monolayer transition metal dichalcogenide semiconductor. arXiv:1404.2331, Nat. Mater. in press.
- [6] Kumar, N., He, J., He, D., Wang, Y. & Zhao, H. Valley and spin dynamics in MoSe₂ two-dimensional crystals. *Nanoscale*, **6**, 12690 (2014).
- [7] Kumar, N. *et al.* Exciton-exciton annihilation in MoSe₂ monolayers. *Phys. Rev. B* **89**, 125427 (2014).
- [8] Mermin, N. D. & Wagner, H. Absence of ferromagnetism or antiferromagnetism in one- or two-dimensional isotropic Heisenberg models. *Phys. Rev. Lett.* **17**, 1133-1136 (1966).
- [9] Bhattacharya, P. *et al.* Room temperature electrically injected polariton laser. *Phys. Rev. Lett.* **112**, 236802 (2014).
- [10] Horzum, S. *et al.* Phonon softening and direct to indirect band gap crossover in strained single-layer MoSe₂. *Phys. Rev. B* **87**, 125415 (2013).
- [11] Jin, Z., Li, X., Mullen, J. T. & Kim, K. W. Intrinsic transport properties of electrons and holes in monolayer transition-metal dichalcogenides. *Phys. Rev. B* **90**, 045422 (2014).
- [12] Ogawa, S., Imada, M., Yoshimoto, S., Okano, M. & Noda, S. Control of light emission by 3D photonic crystals. *Science* **305**, 227-229 (2004)
- [13] Noda, S., Fujita, M., & Asano, T. Spontaneous-emission control by photonic crystals and nanocavities. *Nature Photon.* **1**, 449-458 (2007).
- [14] Jiang, J. H. & John, S. Photonic crystal architecture for room temperature equilibrium Bose-Einstein condensation of exciton-polaritons. *Phys. Rev. X* **4**, 031025 (2014).
- [15] Chamlagain, B. *et al.* *ACS Nano* **8**, 5079-5088 (2014)
- [16] Wang, X. *et al.* Chemical vapor deposition growth of crystalline monolayer MoSe₂. *ACS Nano* **8**, 5125-5131 (2014).
- [17] Shim, G. W. *et al.* Large-area single-layer MoSe₂ and its van der Waals heterostructures. *ACS Nano* **8**, 6655-6662 (2014).
- [18] John, S. & Yang, S. Electromagnetically induced exciton mobility in a photonic band gap.

Phys. Rev. Lett. **99**, 046801 (2007).

[19] Yang, S. & John, S. Exciton dressing and capture by a photonic band edge. *Phys. Rev. B* **75**, 235332 (2007).

[20] Kavokin, A. V. & Malpuech, G. *Cavity polaritons* (Elsevier, Amsterdam, 2003), chap. 3.